Simulations of Viscous Suspension Flows with a Meshless MLS Scheme

Amanda Howard [1] Martin Maxey [1] Nathaniel Trask[2]

[1]Division of Applied Mathematics, Brown University

[2]Sandia National Laboratories

February 28, 2017

Force Coupling Method (FCM) for Stokes Flow: Bidispersed results

- Developing Poiseuille flow in a channel.
- Flux migration, counter to $\nabla\phi$ but in direction of decreasing shear
- Σ^P_{22} creates a "body force" driving the flux
- Interested in the role of forces driving the migration (contact force versus lubrication) and instantaneous dynamics
- How does this change when the particles are different sizes?

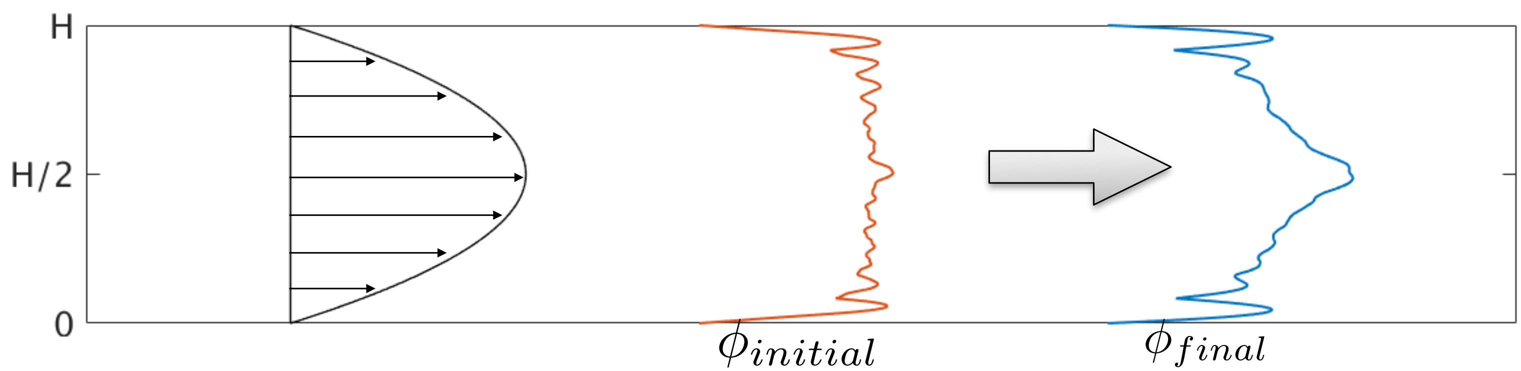

Force Coupling Method (FCM) for Stokes Flow: Bidispersed results

$\phi_L = 30\%,\ \phi_S = 10\%$

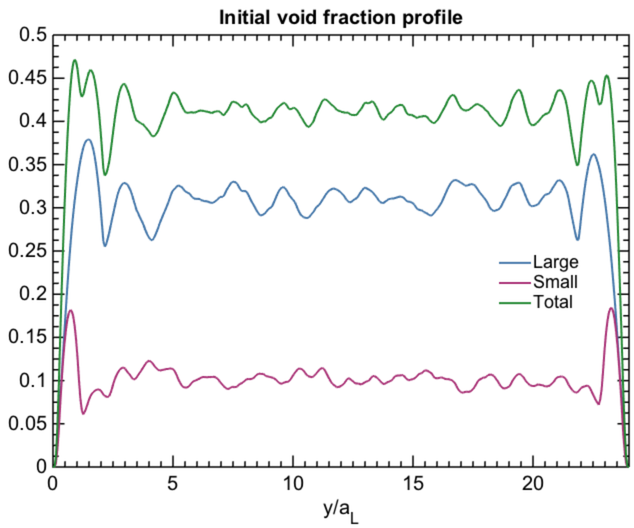

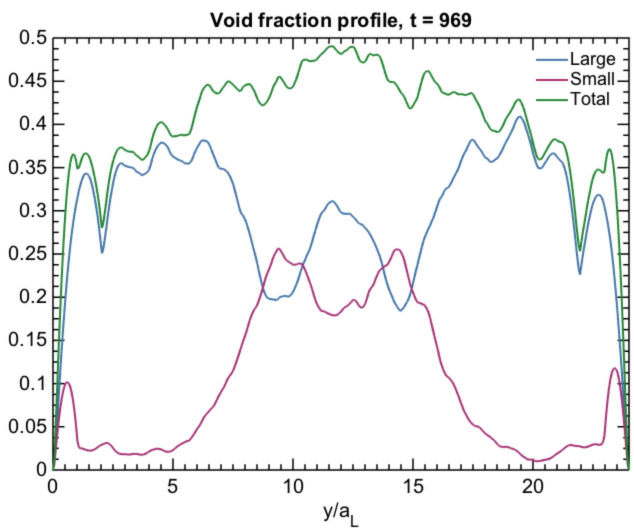

$\phi_L = 10\%,\ \phi_S = 30\%$

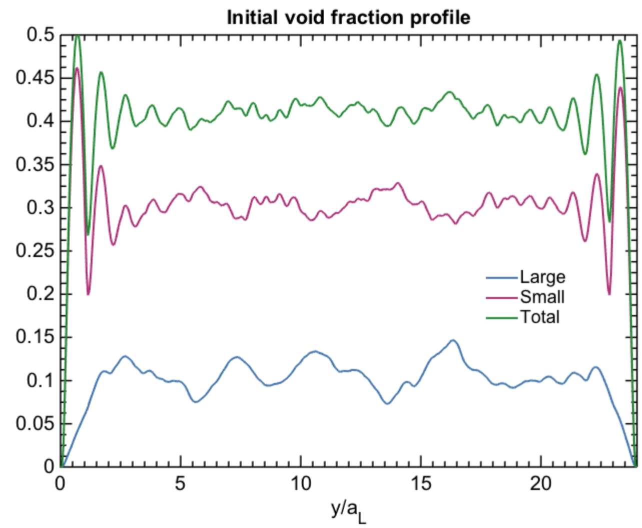

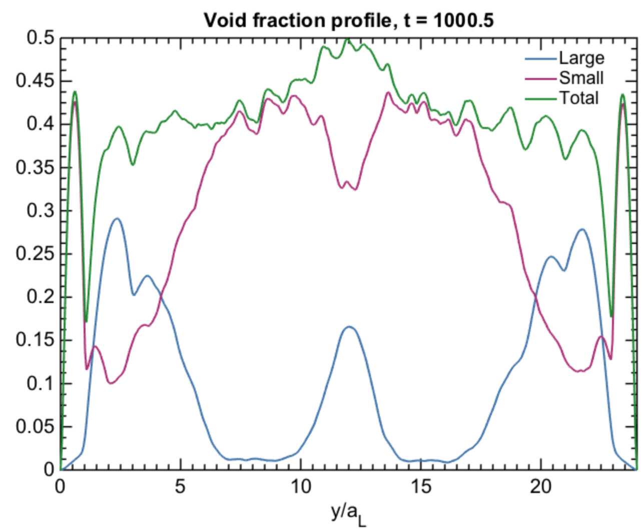

- Uses low-order force multipole expansions to represent the particles.

$$\begin{aligned}
\nabla p &= \mathbf{f}^D + \mu \nabla^2 \mathbf{u} + \sum_{n=1}^{N_p} \{\mathbf{F}^n \Delta_M(\mathbf{r}^n) + (G^n \cdot \nabla)\Delta_D(\mathbf{r}^n)\} \\
\nabla \cdot \mathbf{u} &= 0 \\
\Delta_M(\mathbf{r}) &= \frac{1}{(2\pi\sigma_M^2)^{3/2}} \exp\left(-\frac{r^2}{2\sigma_M^2}\right), \sigma_M = a/\sqrt{\pi} \\
\Delta_D(\mathbf{r}) &= \frac{1}{(2\pi\sigma_D^2)^{3/2}} \exp\left(-\frac{r^2}{2\sigma_D^2}\right), \sigma_D = a/(6\sqrt{\pi})^{1/3}
\end{aligned}$$

- Translational and angular velocities obtained from weighted volume integrals.

$$\mathbf{V}_i = \int (u)_i(\mathbf{x})\Delta_M(\mathbf{r}) d^3\, \mathbf{x},\ \Omega_i = \int \epsilon_{ijk} \frac{\partial \mathbf{u}_k}{\partial \mathbf{x}_j}(\mathbf{x})\Delta_D(\mathbf{r})\ d^3\mathbf{x}.$$

- Mobility problem:

$$\begin{bmatrix} U - U^\infty \\ \Omega - \Omega^\infty \\ -E^\infty \end{bmatrix} = M^{FCM} \begin{bmatrix} F \\ T \\ S \end{bmatrix}$$

- Short range contact forces
- Lubrication viscous forces: Pairwise addition of two-body resistance matrices[1]
- Use preconditioned conjugate gradient method for solving R^{-1} terms. Two steps: outer iteration for FCM dipole terms, inner iteration for local lubrication forces and torques–important for closely clustered particles.[2]
- **Condition number of $\mathcal{R}$ scales like $10^3/\epsilon$.**
- **Condition number of M_{SE} scales like $(a_L/a_s)^3$**

$$
\begin{aligned}
\mathbf{F}^{Lub} &= \mathcal{R}\mathbf{U} \\
\mathbf{U}^T &= (\mathbf{V}^T, \Omega^T) \\
\mathcal{R} &= \begin{bmatrix} R_{VF} & R_{\Omega F} \\ R_{VT} & R_{\Omega T} \end{bmatrix} \\
\begin{bmatrix} U - U^\infty \\ \Omega - \Omega^\infty \\ -E^\infty \end{bmatrix} &= M^{FCM} \begin{bmatrix} F \\ T \\ S \end{bmatrix}
\end{aligned}
$$

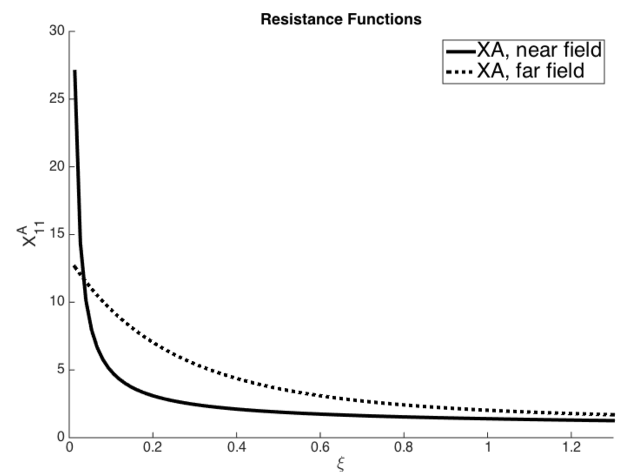

FIGURE: Sample resistance functions[3]. $\xi = \epsilon/\langle a \rangle$

[1] Brady & Bossis, Ann. Rev. Fluid Mech. 20 (1998)
[2] Yeo & Maxey, J. Fluid Mech. 682 (2011)
[3] Jeffrey & Onishi, J. Fluid Mech. 139 (1984)

Moving Least Squares (MLS) basic idea

We want to approximate a function u near a point x_i. Define

$$u_h(x; x_i) = q^*(x_i)$$

where q^* is the solution to a weighted l_2 optimization problem:

$$q^* = \arg\min_{q \in \pi_m} \sum_{i=1}^{N} [u(x_j) - q(x_j)]^2 W_{ij}$$

Operator D^α is found by applying D^α to the reconstruction:

$$D^\alpha \mathbf{u}_i \approx D_h^\alpha \mathbf{u}_i := D^\alpha q^*(\mathbf{x}_i)$$

MLS for Stokes Flow[4]

- Recently developed Staggered MLS scheme for numerical solutions of Stokes flow
- Polynomial interpolants are used to represent the flow using least squares minimization
- High order accurate (4th or 6th order easily obtained by changing the order of the polynomial interpolants.)
- Force-free and torque-free colloids with position $\mathbf{X}_i$, orientation Θ_i, and boundary $\partial\Omega_i$.

$$\begin{cases} -\nu\nabla^2\mathbf{u} + \nabla p = \mathbf{f} & \mathbf{x} \in \Omega \\ \nabla \cdot \mathbf{u} = 0 & \mathbf{x} \in \Omega \\ \mathbf{u} = \mathbf{w} & \mathbf{x} \in \partial\Omega \\ \mathbf{u} = \dot{\mathbf{X}}_i + \dot{\Theta}_i \times (\mathbf{x} - \mathbf{X}_i) & \mathbf{x} \in \partial\Omega_i \end{cases}$$

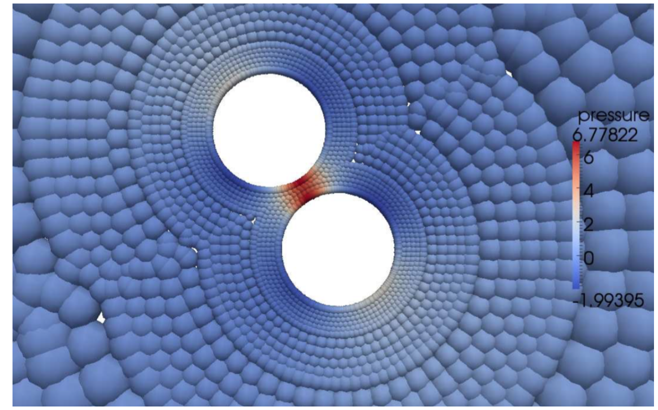

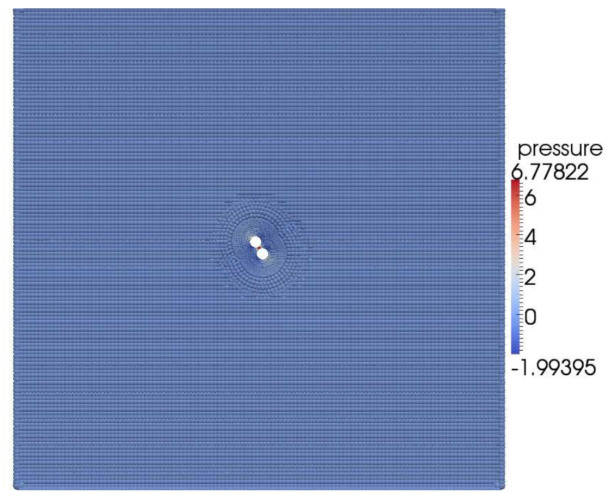

Figure: Point adaptivity for colloids interacting under shear flow. Particle adaptivity visualized by rendering spheres at each point with diameter proportional to ϵ_i

[4] N. Trask, Ph.D. thesis (2015)

Choose **u** in the space of divergence free vector fields.

$$\begin{cases} \nu \nabla \times \nabla \times \mathbf{u} + \nabla p = \mathbf{f} & \mathbf{x} \in \Omega \\ \mathbf{u} = \mathbf{w} & \mathbf{x} \in \partial\Omega \end{cases}$$

$$\begin{cases} \nabla^2 p = \nabla \cdot \mathbf{f} & \mathbf{x} \in \Omega \\ \partial_n p + \nu \hat{\mathbf{n}} \cdot \nabla \times \nabla \times \mathbf{u} = \hat{\mathbf{n}} \cdot \mathbf{f} & \mathbf{x} \in \partial\Omega \end{cases}$$

$$\begin{cases} \mathbf{u} = \dot{\mathbf{X}}_i + \dot{\Theta}_i \times (\mathbf{x} - \mathbf{X}_i) & \mathbf{x} \in \partial\Omega_i \\ m_i \ddot{\mathbf{X}}_i = \int_{\partial\Omega_i} \sigma_v \cdot \, dA & \\ I_i \ddot{\Theta}_i = \int_{\partial\Omega_i} (\mathbf{x} - \mathbf{X}_i) \times \sigma_v \cdot \, dA & \end{cases}$$

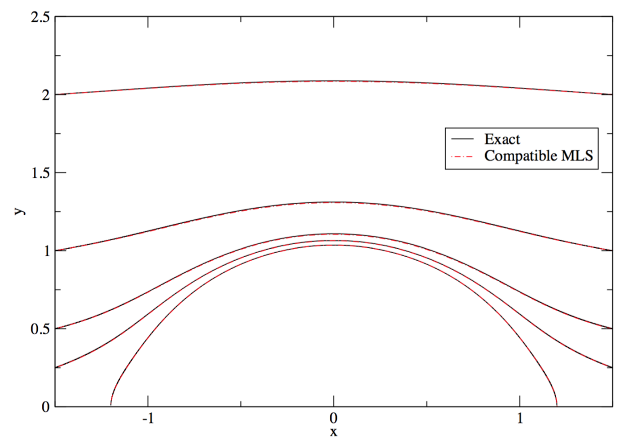

Figure: Exact and MLS results for trajectory of particles in shear flow for varying initial colloid configuration.

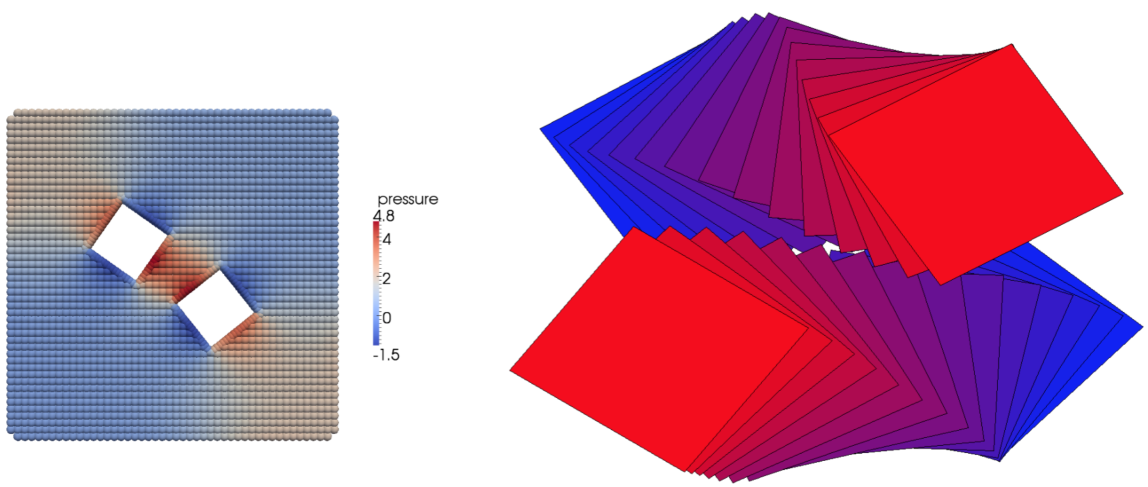

Figure: Square particles of unit size in shear flow.

MLS Discretization

- Identify a virtual dual face with each edge and a virtual cell with each node.

$$div_h : E \to N$$

$$grad_h : N \to E$$

$$grad_h(\phi)_{ij} = \int_{e_{ij}} \nabla\phi \cdot ds = \phi_j - \phi_i$$

- To define div_h, first define the radial component function $\mathbf{u}_{i\to}(\mathbf{x}) := \mathbf{u}(\mathbf{x}) \cdot 2(\mathbf{x} - \mathbf{x}_i)$.
- For sufficiently smooth $\mathbf{u}$, $\mathbf{u}(\mathbf{x}_i) = \frac{1}{2}\nabla\mathbf{u}_{i\to}(\mathbf{x}_i)$ and $\nabla \cdot \mathbf{u}(\mathbf{x}_i) = \frac{1}{4}\nabla \cdot \nabla\mathbf{u}_{i\to}(\mathbf{x}_i)$ hold.
- Reconstruct the vector fields and divergences at nodes by sampling component functions at edges:

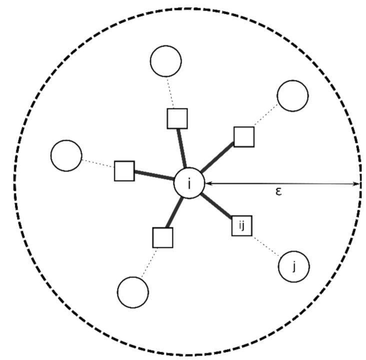

$$q^* = \arg\min_{q \in \pi_m} \left\{ \sum_j \left[\mathbf{u}(\mathbf{x}_{ij}) \cdot 2(\mathbf{x}_{ij} - \mathbf{x}) - q(\mathbf{x}_{ij})\right]^2 W_{ij} \right\}$$

$$\mathbf{u}_h(\mathbf{x}_i) = \frac{1}{2}\nabla q^*(\mathbf{x}_i), \quad \nabla_h \cdot \mathbf{u}(\mathbf{x}_i) = \frac{1}{4}\nabla \cdot \nabla q^*(\mathbf{x}_i)$$

MLS Discretization

- Viscous operator:

$$\nabla \times \nabla \times \mathbf{u}(\mathbf{x}_i) \approx \nabla \times \nabla \times_h \mathbf{u}(\mathbf{x}_i) := \nabla \times \nabla \times \mathbf{v}^*(\mathbf{x}_i)$$

- Standard discretization over this basis:

$$\mathbf{v}^* = \arg \min_{v \in \pi_m^{div}} \left\{ \sum_{j=1}^{N_P} [\mathbf{u}(\mathbf{x}_j) - \mathbf{v}(\mathbf{x}_j)]^2 W_{ij} \right\}$$

- Because of the form of minimizing a polynomial, we can write each quantity as a linear combination:

$$\begin{aligned} \nabla_h^2 p_i &= \sum_{j \in (W_{ij})} \alpha_{ij}^1 p_j \\ \nabla_h p_i &= \sum_{j \in (W_{ij})} \alpha_{ij}^2 p_j \\ \nabla \times \nabla \times_h \mathbf{u}_i &= \sum_{j \in (W_{ij})} \alpha_{ij}^3 \mathbf{u}_j \end{aligned}$$

- Dirichlet boundary conditions are reinforced on the global matrix.
- Lack of symmetry makes it difficult to provide divergence free. Only divergence free in the local polynomial reconstruction.

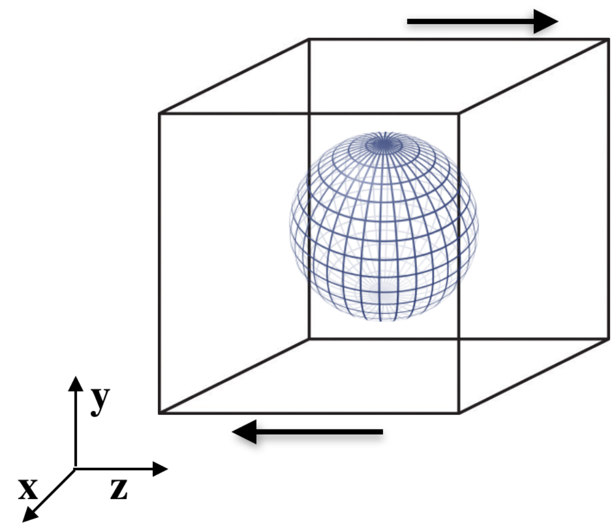

- Sphere with radius r in a box $\Omega = [-1, 1]^3$.
- Boundary conditions: $u = (0, 0, y)$ on $\partial\Omega$.

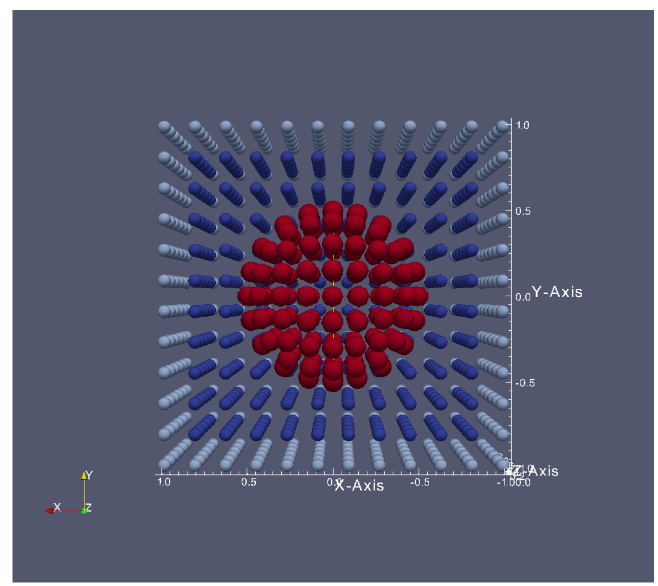

Sphere in Couette flow

$\Omega_x = \frac{1}{2} = 0.5$

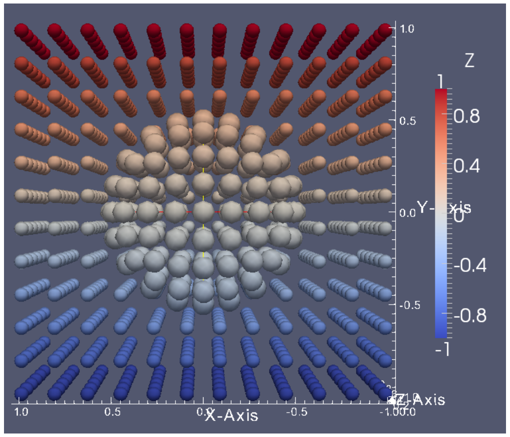

Figure: $N = 12^3, \Omega_x = 0.500684$

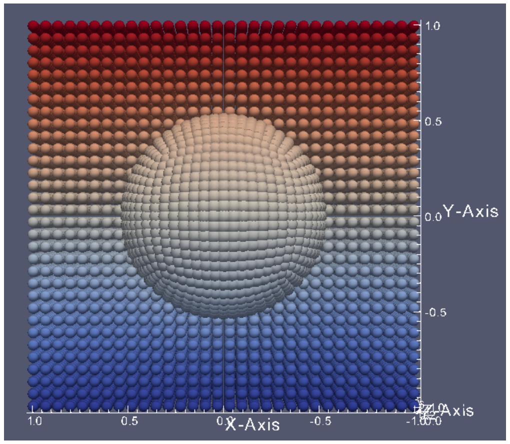

Figure: $N = 32^3, \Omega_x = 0.500149$

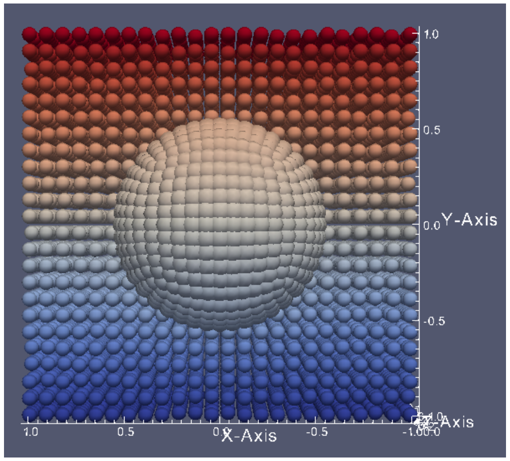

Figure: $N = 24^3, \Omega_x = 0.496785$

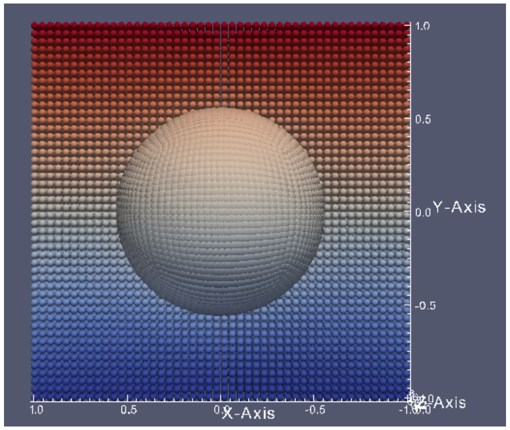

Figure: $N = 48^3, \Omega_x = 0.499069$

- Sphere with radius a in a box $\Omega = [-1, 1]^3$.
- Boundary conditions: $u = (0, 0, 0)$ on $\partial\Omega$.
- Body force $F = (0, -6\pi\mu a U_0, 0)$ imposed on the sphere.

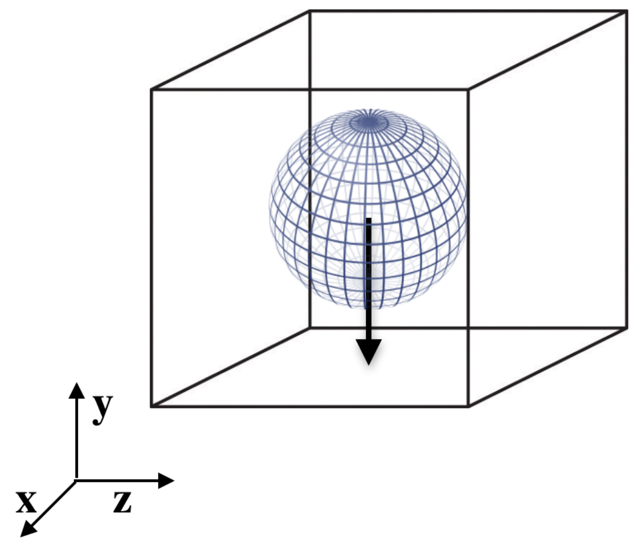

$N = 48^3$

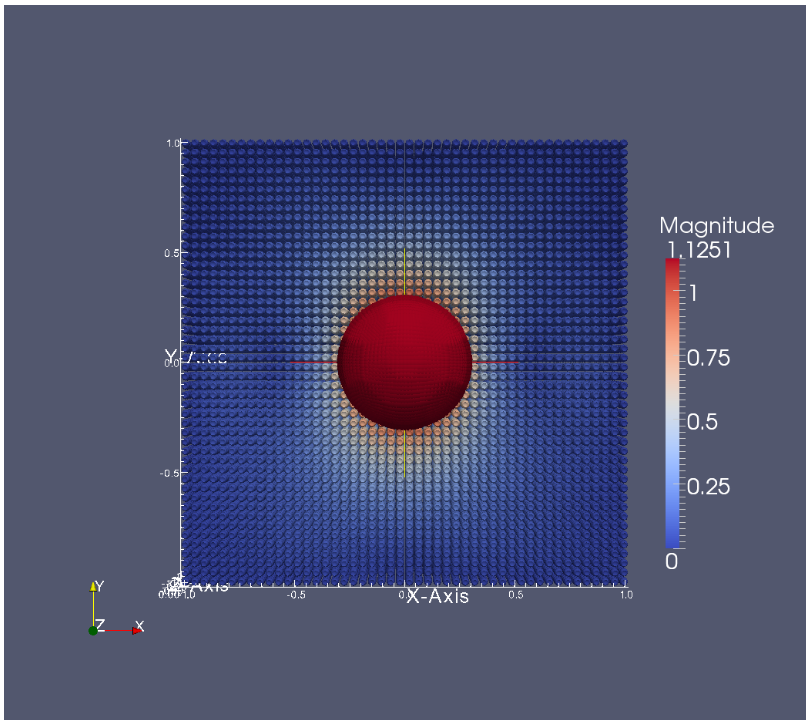
Magnitude
1.1251
1
0.75
0.5
0.25
0
X-Axis
1.0
0.5
-0.5
-0.5
0.5
1.0
Y
Z
X

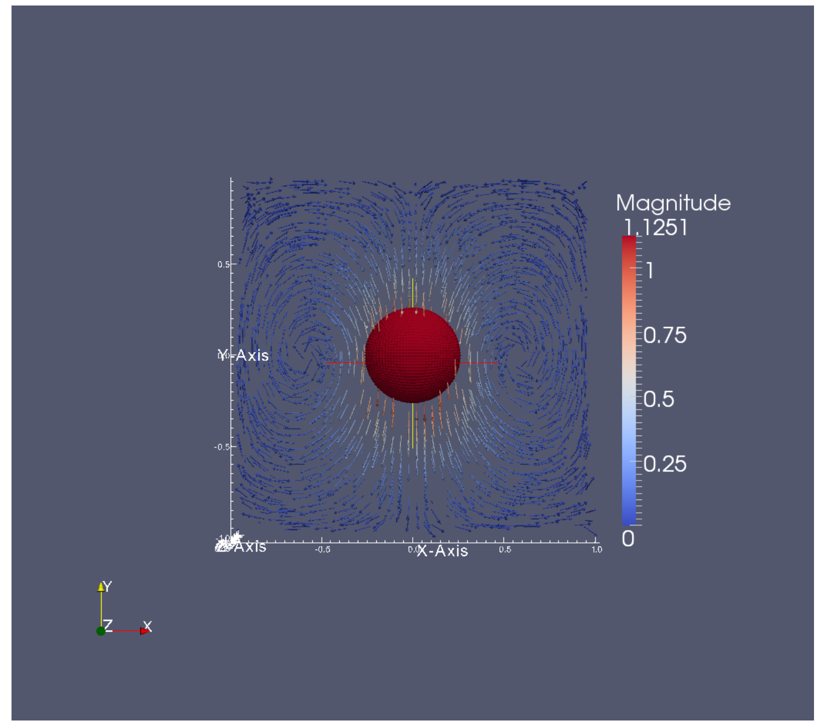
Magnitude
1.1251
1
0.75
0.5
0.25
0
Y-Axis
X-Axis
Y
Z
X

Conclusions

- Have fast and stable methods using only the graph of neighbor connectivity.
- Applications include irregular domains and non-spherical particle shapes with higher order accuracy
- Future work: coupling FCM and MLS

This work is supported by the NSF Graduate Research Fellowship under Grant No. DGE 1058262 and the U.S. Department of Energy Office of Science under Award Number DE-SC0009247.